Eye opening induces a rapid dendritic localization of PSD-95 in central visual neurons

Akira Yoshii*†, Morgan H. Sheng*‡§¶, and Martha Constantine-Paton*‡§‖**

Departments of *Biology and ‡Brain and Cognitive Sciences, §Center for Learning and Memory, ‖McGovern Institute for Brain Research, and ¶Howard Hughes Medical Institute, Massachusetts Institute of Technology, 77 Massachusetts Avenue, Cambridge, MA 02139-4307; and †Department of Neurology, Massachusetts General Hospital, 55 Fruit Street, Boston, MA 02114

Edited by Charles F. Stevens, The Salk Institute for Biological Studies, La Jolla, CA, and approved December 9, 2002 (received for review September 24, 2002)

The membrane-associated guanylate kinase PSD-95 scaffolds *N*-methyl-D-aspartate receptors to cytoplasmic signaling molecules, and associates with other glutamate receptors at central synapses. However, regulation of PSD-95 *in vivo* is poorly understood. We provide evidence of an activity-dependent redistribution of PSD-95 to dendrites in central visual neurons that is tied to eye opening. Six hours after eye opening, increased dendritic PSD-95 coimmunoprecipitates with the same proportions of stargazin, increased proportions of the *N*-methyl-D-aspartate receptor subunit NR2A, and decreased proportions of NR2B. Sustained high levels of PSD-95 in dendrites are dependent on continued pattern vision in juvenile but not mature animals, suggesting that the stabilization of PSD-95 at synapses may be involved in the control of developmental plasticity.

PSD-95 is a PDZ-domain-containing constituent of glutamate postsynaptic densities (PSDs) that directly associates with *N*-methyl-D-aspartate receptors (NMDARs) (1), kainate receptor subunits (2), and with α-amino-3-hydroxy-5-methyl-4-isoxazole propionic acid receptors (AMPARs) via stargazin (3). PSD-95 also holds key participants in other signaling pathways close to the glutamate-gated ion currents thereby providing a major link between glutamate release and postsynaptic signaling (3–6). PSD-95 is believed to be the major scaffolding molecule of mature NMDARs. Here we study how its interactions with NMDARs and other postsynaptic density molecules are regulated by natural increases in activity in the intact developing brain.

Materials and Methods

Animals. All animal manipulations were performed in accord with the guidelines of the Massachusetts Institute of Technology Institutional Animal Care and Use Committee. Litters of Sprague–Dawley rats were kept under 12 h/12 h light/dark cycles except for dark rearing (DR) experiments. Two to three days before EO, eyelids were sutured. On the day of EO, lids were separated under photopic conditions and pups were checked every 15–30 min to ensure that they were awake until sacrifice.

Fractionation. For the developmental survey in Fig. 1, eight pups were used for each age except adult, where three animals were used. Each controlled EO immunoblot experiment (Fig. 2) used three litters, and within each litter three littermates were killed for each time point. Whole lysates were prepared from homogenates in Laemmli buffer by trituration through a 26-gauge syringe needle. Synaptoneurosome (crude neuropil fraction) protein (7–9) and synaptosome (presynaptic vesicle and postsynaptic membrane) protein (10) were prepared as in citations.

Immunoblotting. Immunoblotting was performed as previously described (11). Antibodies used were: anti-PSD-95 (catalog no. 05-494, Upstate Biotechnology), anti-SAP102 (5′ 2d3, a gift from C. Garner), anti-GKAP (c9589, ref. 12), anti-α-CAMKII (catalog no. MA1-048, Affinity Bioreagents, Neshanic Station, NJ) and anti-GSK3β (catalog no. G22320, Transduction Laboratories, Lexington, KY). Band densities were quantified with NIH IMAGE. Three gels from each protein isolation were used to substantiate findings for each experiment. Fold changes at each time point were calculated relative to the protein level at 0 h on the same gels. Results are reported as averages ± SEM. Data points were considered significant changes from the 0 h level at the $P < 0.05$ if their 95% confidence intervals given as mean ± (1.96 × SEM) fell above 1.0-fold. When GKAP95 and PSD-95 had to be examined on the same lanes, blots were probed with anti-GKAP first, stripped completely, then probed again with PSD-95. There was no cross-reactivity between the anti-PSD-95 and anti-GKAP antibodies.

Immunocytochemistry. After 4% paraformaldehyde perfusion and vibratome sectioning at 50 μm, coronal brain sections were permeabilized in PBS containing 1% Triton X-100 at room temperature for 10 min. Sections were reacted overnight with mouse anti-PSD-95 at room temperature. After rinsing, sections were incubated in biotinylated anti-mouse secondary antibody (Jackson ImmunoResearch) and Cy5-streptavidin (Jackson ImmunoResearch) (13). When double staining, incubation with microtubule-associated protein 2 (MAP2) antibody (catalog no. AB5622 ×100, Chemicon) overnight at room temperature, and then with anti-rabbit Alexa Fluor 546 (Molecular Probes) followed. Images were captured at ×600 (Fig. 3 *A–G*), and ×400 (Fig. 3 *H*, *I*, *K*, and *L*) under identical settings with a Nikon PCM 2000 confocal microscope. The *Z* series of optical sections taken at intervals of 0.5 μm through 6 μm of tissue were reconstructed. Stacks of images were collected at equivalent rostrocaudal/mediolateral positions in the superficial layers of the superior colliculus (sSC). For quantification, images were imported into NIH IMAGE (http://rsb.info.nih.gov/nih-image/). Quantification was performed as described (14). Threshold was determined to maximize pixels with in-focus fluorescence for all sections to be compared, and images were digitized. This threshold was set after examining sections from multiple pups in the litter and was retained for analyses of all sections from that litter. Thresholds were ≈6-fold greater than the background fluorescence. In each image of sSC, four volumes (144 pixels × 144 pixels, where each pixel represents a 0.3 μm × 0.3 μm × 6 μm volume of tissue) were randomly sampled at equivalent levels of coronal sections of the sSC for each littermate killed either with or without EO. The number of pixels containing PSD-95 immunoreactivity in these equal volumes of tissue from each animal was determined. These numbers were divided into the before and after EO groups to obtain the average and standard error of labeled pixels divided by the fixed sample volume (labeled pixel density, LPD) for each

This paper was submitted directly (Track II) to the PNAS office.

Abbreviations: sSC, superficial layer of superior colliculus; VC, visual cortex; NMDAR, *N*-methyl-D-aspartate receptor; AMPAR, α-amino-3-hydroxy-5-methyl-4-isoxazole propionic acid receptor; PSD, postsynaptic density; DR, dark rearing; LPD, labeled pixel density; wl, whole lysates; P*n*, postnatal day *n*; EO, eye opening.

**To whom correspondence should be addressed. E-mail: mcpaton@mit.edu.

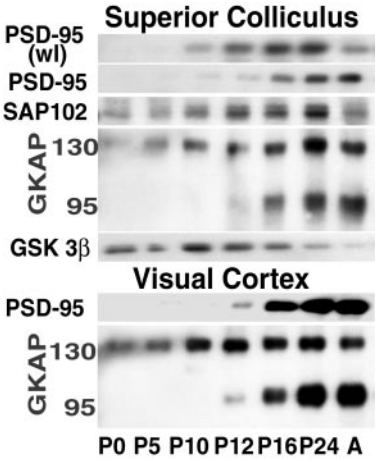

Fig. 1. PSD-95 and GKAP95 increase in synaptoneurosomes from sSC and VC in the interval surrounding EO. PSD-95 increases gradually in wl of the sSC from P10 through P24 with some decrease in adulthood. Synaptoneurosomal PSD-95 increased abruptly between P12 and P16. In contrast, SAP102, examined on the same blots, is present in the sSC synaptoneurosome fractions from P0 and its level increases gradually with a drop in the adult (A). The two families of GKAP splice variants also increase in synaptoneurosome fractions from the sSC. The 95-kDa isoforms follow PSD-95 levels, whereas 130-kDa variants follow SAP102 levels. The same changes are observed in protein from VC synaptoneurosomes.

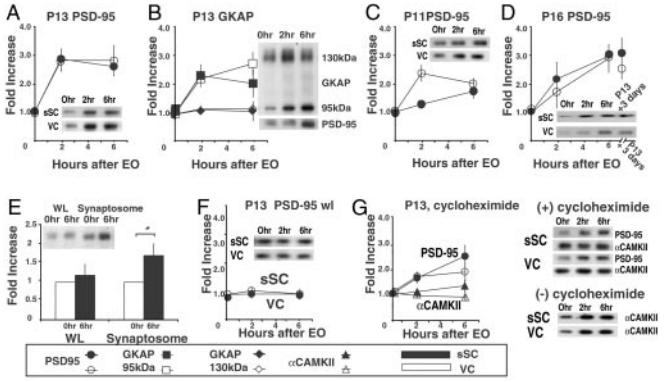

Fig. 2. Rapid increases in PSD-95 synaptoneurosome are tied to EO, not age, and the increases appear to be caused by redistribution, not translation. The density of each band at 2 and 6 h is shown as a ratio relative to band density from littermates killed at the same age without EO (0 h). (*A*) In both sSC and VC increased PSD-95 synaptoneurosome levels increase at 2 and 6 h after EO when controlled EO is performed on P13, the normal day of EO (95% confidence intervals at 6 h, sSC: 2.59 ± 0.63, VC: 2.80 ± 1.02). (*B*) Levels of GKAP95 increase after EO on P13 with the same timing as PSD-95, whereas levels of GKAP130 on the same gels remain constant (GKAP 95, 95% confidence intervals at 6 h, sSC: 1.83 ± 0.70, VC: 2.76 ± 0.77; GKAP130, 95% confidence intervals at 6 h, sSC: 1.09 ± 0.49, VC: 1.19 ± 0.21). (*C* and *D*) Levels of PSD-95 in synaptoneurosomes from sSC and VC also increase 2 and 6 h after EO at P11 (95% confidence intervals at 6 h, sSC: 1.74 ± 0.48, VC: 2.02 ± 0.34) and P16 (95% confidence intervals at 6 h, sSC: 3.04 ± 0.71, VC: 2.96 ± 0.98). In *D*, the last data point represents the level of PSD-95 in littermates that opened their eyes at the normal time (P13) and were killed 3 days later. (*E*) Synaptosome fractions also show increases of PSD-95 6 h after EO (95% confidence intervals at 6 h, wl: 1.14 ± 0.15, synaptosome: 1.54 ± 0.27). (*F*) No change in PSD-95 level is observed 2 or 6 h after EO in wl from sSC and VC of P13 animals (95% confidence intervals at 6 h, sSC: 0.98 ± 0.36, VC: 1.02 ± 0.36). (*G*) Cycloheximide does not block the PSD-95 protein increase in synaptoneurosomes (95% confidence intervals at 6 h, sSC: 2.45 ± 0.83, VC: 1.76 ± 0.68), whereas it does block α-CAMKII synthesis (confidence intervals at 6 h, sSC: 1.21 ± 0.31, VC: 0.90 ± 0.153), which normally increases significantly because of local synaptic synthesis after EO. Representative gels are shown at left. (Quantitation of α-CAMKII increase in untreated animals not shown.) All error bars indicate SEM.

treatment in each litter (Fig. 3*J*). For analyses comparing monocular eye zones in dLGNs of the same animals (Fig. 3 *K–M*), the same method of obtaining labeled pixel density was applied. For details, see *Supporting Text*, which is published as supporting information on the PNAS web site, www.pnas.org.

Immunoprecipitation. Synaptoneurosome protein from both the sSC and visual cortex (VC) of 10 animals was immunoprecipitated with anti-PSD-95 to examine coprecipitated NR2 proteins (anti-NR2A, Upstate Biotechnology catalog no. 06-313; anti-NR2B, Transduction Laboratories catalog no. N38120). Coimmunoprecipitates of anti-PSD-95 antibody were also probed with the anti-stargazin antibody (Calbiochem catalog no. 681517). The bands on probe gels were quantified as above and values for particular molecules were calculated as ratios relative to the PSD-95 band on the same lane.

Results

In an immunoblot survey, changes in levels of various sSC PSD proteins were examined. Immunoreactivity for PSD-95 was present in whole lysates (wl) of sSC by P10, gradually increased during development and dropped in adulthood (Fig. 1). However, in corresponding synaptoneurosome fractions, PSD-95 levels rose significantly around EO (postnatal day, P12–P16) and remained high in the adult. In the same fractions, another membrane-associated guanylate kinase family protein known to bind NMDARs, SAP102 (15), increased earlier, did not show a pronounced change in level at EO, and decreased in the adult. The 130- and 95-kDa species of GKAP, two families of at least five splice variants (12, 16), increased in the same synaptoneurosomes during the postnatal period but only GKAP95 isoforms showed a rapid increase coinciding with the change in PSD-95. GSK-3β is shown because it decreased in the same synaptic fractions. PSD-95 and GKAP95 were subsequently examined by using the same protocol on VC and also showed significant synaptoneurosome increases around EO.

EO Induces Dendritic PSD-95 Increases. Rat pups open their eyes around P13. To determine whether EO caused PSD-95 increases in dendrites we compared synaptoneurosome protein levels in P11, P13, and P16 pups before EO (0 h) at 2 and 6 h after EO. We controlled EO by suturing eyelids. Within 2 h of EO at P13, the level of PSD-95 increased significantly (Fig. 2*A*). On the same blotting membranes, GKAP95 increased within 2 h, whereas GKAP130 remained constant (Fig. 2*B*). A significant, though smaller, rise of PSD-95 in synaptoneurosomes was seen at P11, when the eyes were opened prematurely (Fig. 2*C*). At P16, the PSD-95 increase at 6 h was not only significant but also close to levels seen in P16 littermates who had had their eyes open for 3 days (P13 EO + 3 days; Fig. 2*D*).

We also examined synaptosome fractions considerably more enriched for PSD molecules than synaptoneurosomes (10). PSD-95 increased significantly 6 h after EO in P13 synaptosome preparations from pooled sSC and VC tissue. The synaptosome increase was less prominent than that seen in synaptoneurosomes (Fig. 2 *A* and *E*), perhaps because some of the PSD-95 appearing rapidly in dendritic fractions is not immediately incorporated at postsynaptic membranes.

Rapid Dendritic Redistribution of PSD-95. Rapid EO-dependent increases in PSD-95 could result from local synthesis of new protein or a shift in the intracellular distribution of existing protein. Levels of PSD-95 in wl showed no significant changes after EO (Fig. 2*F*). Nevertheless, the possibility of local translation was examined directly by using i.p. injections of cyclohex-

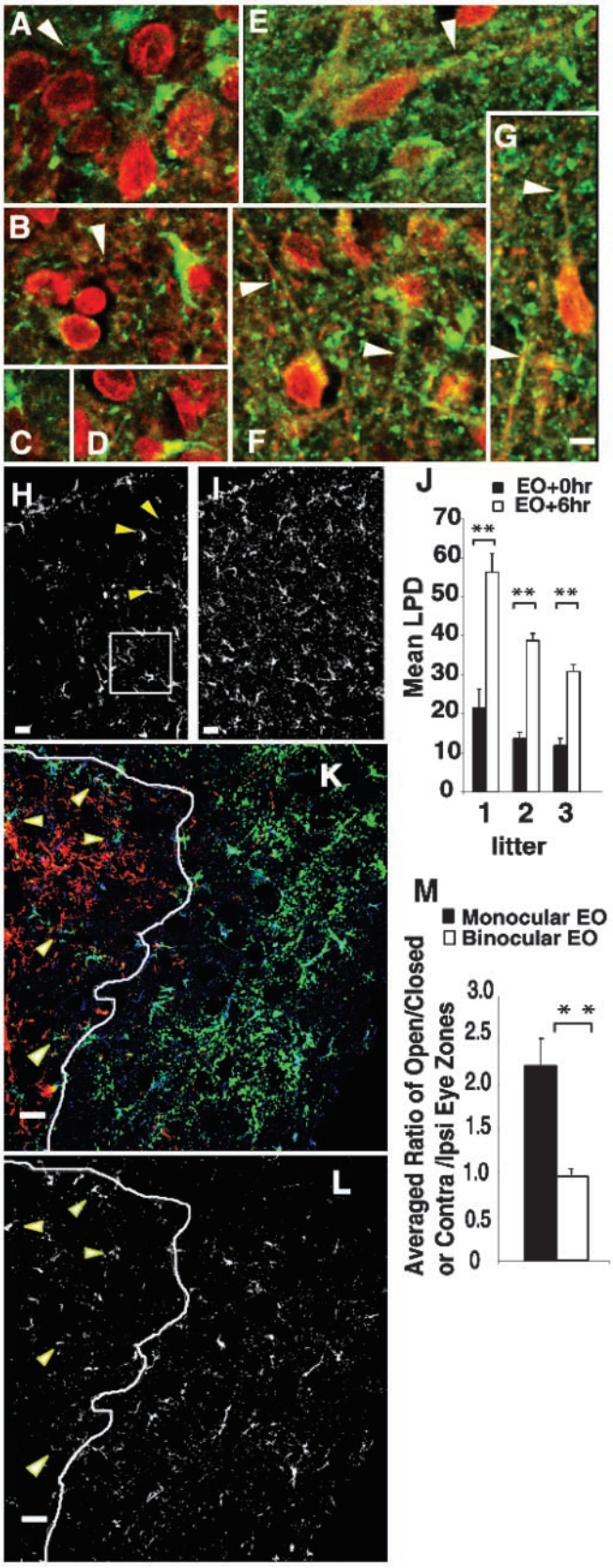

Fig. 3. PSD-95 becomes localized along sSC dendrites after EO. (*A–D* and *H*) Before EO on P13, confocal reconstructions of sSC coronal sections show PSD-95 immunoreactivity (green) as large concentrations in the soma and proximal dendrites identified with anti-MAP2 (red). (*A* and *B*) Arrows indicate segments of MAP2-labeled dendrites running longitudinally within the confocal reconstructions. (*H*) Arrowheads show PSD-95 immunoreactivity in perinuclear cytoplasm. (*E–G* and *J*) Equivalent reconstructions from littermates killed 6 h after EO at P13 show punctate label distributed along longitudinally viewed dendrites (arrows) as well as many small puncta in the neuropil probably reflecting label in dendrites cut in cross-section. This punctate labeling pattern is characteristic of PSD-95 staining at synapses. (*I*) In the lower power views from another set of littermates, the PSD-95 change with EO is seen as an increase in small puncta dispersed throughout the neuropil. (*J*) The density of pixels with any PSD-95 immunoreactivity (LPD) was increased nearly 2-fold in reconstructions at EO + 6 h (*I*) compared with littermates with unopened eyes (EO + 0 h, *H*). All differences were significant (paired sample Student's *t* test; **, $P < 0.01$). Error bars indicate SEM. (*K*) Monocular EO at P13 induces more dendritic PSD-95 in the open eye as compared with the closed eye termination zone of the dLGN. Open eye input is green, closed eye input is red, and PSD-95 immunoreactivity is blue. The margin between the zones of each eye is shown as a white line. These zones of segregation are not absolute. (*L*) PSD-95 label alone. Arrowheads point to five open eye axons within the closed eye zone that are juxtaposed to heavy PSD-95 immunoreactivity. (*M*) Average of the PSD-95 LPD ratios between open and closed eye or contra- and ipsilateral eye termination zones. A significant increase (paired *t* test; **, $P < 0.01$) in the open eye area in animals with monocular EO, suggesting more dispersion of PSD-95 in the open eye zone, despite the fact that PSD-95 immunoreactivity adjacent to open eye axons in the closed eye zone is not taken into account in this assay. No differences in PSD-95 LPD are observed between the two zones in animals with binocular EO (paired *t* test, $P = 0.2$). Error bars indicate SEM. (All scale bars = 10 μm.)

imide (1.0 mg/kg) 1 h before EO at P13 (17). Synaptoneurosomes from the sSC and VC of these pups continued to show significant increases in PSD-95 levels 2 and 6 h after EO (Fig. 2*G*), though levels were decreased relative to untreated pups. Therefore, to examine the effectiveness of the cycloheximide treatment, we probed the same membranes for the α subunit of Ca^{2+} calmodulin kinase II (α-CAMKII), which shows increased local synthesis at synapses with increased activity in the hippocampus (18, 19), sSC (20), and VC (21). α-CAMKII increased significantly within 6 h of EO (Fig. 2*G Bottom*, quantification not shown) in synaptoneurosomes from untreated pups. Nevertheless, α-CAMKII levels did not change from littermates with unopened eyes in the presence of cycloheximide (Fig. 2*G*).

Immunocytochemical Localization of PSD-95. To visualize PSD-95 protein in sections from sSC six littermates from three litters were killed on P13 without EO or at 6 h after EO. Vibratome sections were reacted for PSD-95 and MAP2, a marker for large dendrites and neuronal cell bodies. Before EO, aggregates of PSD-95 were preferentially localized to cell bodies and proximal dendrites. The neuropil and isolated dendrites showed only sparse puncta (Fig. 3 *A–D*). In contrast, PSD-95 reactivity was dispersed in somal and dendritic cytoplasm 6 h after EO, giving a green hue to much of the cytoplasm in the merged images (Fig. 3 *E–G*). In addition, many relatively small PSD-95 puncta were distributed on, or closely adjacent to, large dendritic branches (Fig. 3 *E–G*, arrowheads). The puncta that did not directly overlap with MAP2-labeled processes were probably localized to fine dendrites or dendritic spines, which contain few microtubules and cannot be observed with MAP2. The many additional small puncta appearing throughout the neuropil may represent PSD-95 in small dendrites running perpendicular to the plane of section.

Comparisons between the average number of pixels containing any PSD-95 immunoreactivity were made in fixed volumes of sSC tissue from littermates without and after EO (square in Fig. 3*H*). Four pups from each of three litters were killed on P13, two before EO and two 6 h after EO. The mean number of PSD-95-labeled pixels (mean LPDs) before and after EO for each litter (Fig. 3 *H–J*) showed a 2- to 2.5-fold increase in PSD-95 dispersion after, as compared with before EO (Fig. 3*J*). We also examined the dLGN of P13 pups by using

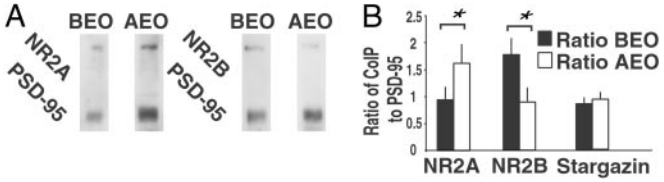

Fig. 4. EO induces rapid synaptosome increases in PSD-95 bound NR2A subunits and decreases in PSD-95 bound NR2B subunits. (*A*) Different amounts of NR2 subunits coimmunoprecipitate with the PSD-95 antibody before (BEO) and 6 h after EO (AEO) at P13. (*B*) Quantification of changes in the proportion of NR2A ($n = 4$ blots) and NR2B ($n = 5$ blots) subunits coimmunoprecipitating with PSD-95 AEO as compared with BEO (paired Student *t* test; ⋆, $P < 0.05$). Identical results were obtained with protein from VC (data not shown). Data were normalized against optical density measurements for PSD-95-immunoreactive bands detected on the same gels. The proportion of stargazin immunoprecipitating with PSD-95 was unchanged ($n = 4$, paired Student *t* test, $P = 0.274$). Error bars indicate SEM.

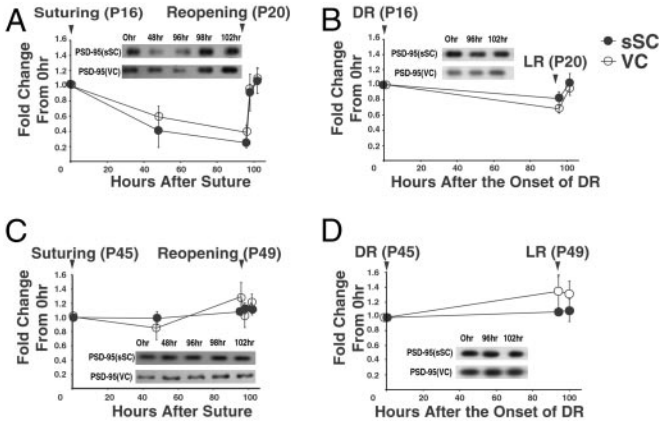

Fig. 5. Synaptoneurosomal PSD-95 levels decrease reversibly with deprivation of pattern vision in developing but not mature rats. (*A*) Four days of eye closure, starting at P16 after 3 days of pattern vision, decreases synaptoneurosome PSD-95 (95% confidence intervals at 96 h, sSC: 0.25 ± 0.13, VC: 0.38 ± 0.20). Levels increase rapidly at 2 and 6 h after eye reopening. (*B*) Four days of DR caused a significant decrease in the synaptoneurosome level of PSD-95 (95% confidence intervals at 96 h, sSC: 0.81 ± 0.17, VC: 0.68 ± 0.11) but the decrease was smaller than that seen with eyelid suturing (LR, light rearing). A separate series of blots were performed on wl from similarly treated animals. No significant differences in PSD-95 protein levels were observed at any interval (data not shown). (*C* and *D*) The same deprivation and EO protocols do not change levels of dendritic PSD-95 in young adult rats (95% confidence intervals at 96 h eye suture, sSC: 1.08 ± 0.10, VC: 1.28 ± 0.35; 95% confidence intervals at 96 h dark-rearing, sSC: 1.08 ± 0.12, VC: 1.39 ± 0.48). All error bars indicate SEM.

a monocular EO paradigm and cholera toxin to mark axons from an open versus a closed eye in the same section. The dispersion of PSD-95 label was significantly increased in zones receiving activity from an open as compared with a closed eye. No differences in ipsilateral or contralateral eye zone LPDs were observed in littermates when both eyes were opened at the same time (Fig. 3 *K–M*).

PSD-95 and Glutamate Receptors. We determined whether PSD-95 targeted to dendrites after EO is associated with more NR2A than the PSD-95 present in the dendrites before EO. PSD-95 was immunoprecipitated from synaptoneurosome fractions before and 6 h after EO. More NR2A precipitated with PSD-95 after than before EO (Fig. 4). Conversely, more NR2B precipitated with PSD-95 before as compared with after EO (Fig. 4). Similar complementary changes were observed in synaptoneurosomes from VC (data not shown). Thus, the PSD-95 that is targeted to dendrites with EO appears to increase the proportion of NR2A in PSD-95-associated NMDARs. Stargazin coimmunoprecipitating with PSD-95 increased after EO. However, the proportion of stargazin immunoreactivity to PSD-95 immunoreactivity on the same lane remained constant before and after EO (Fig. 4*B*).

Developmental Lability of PSD-95 Levels. The rapid increase in synaptoneurosome and synaptosome levels of PSD-95 with EO motivated us to ask whether this change was stable. Eyes of 10 littermates that opened their eyes at P13 were shut again at P16. Two animals were killed before eyelid suturing, two after 2 days and two after 4 days of survival in normal light/dark cycles with eyelids reclosed. The remaining four pups had eyelids opened again after the 96-h period of suture and were allowed to survive for 2 or 6 additional hours. The level of PSD-95 in the synaptoneurosome fractions from the littermates killed at P16 without lid suture (0 h) served as a baseline. Levels of PSD-95 showed a steady decrease over the 4-day period of survival in the animals with lid suture. Data from the 96-h interval were significantly reduced from baseline. Nevertheless, littermates that survived for 2 or 6 h after reopening their eyes at P20 showed a rapid return to the level of synaptoneurosome PSD-95 exhibited by their littermates at P16 (Fig. 5*A*). The increase from the lid-sutured 96-h interval was ≈2- to 2.5-fold, roughly the same increase seen on initial EO in Fig. 1 and 2. Thus, visual activity is important in keeping levels of PSD-95 high in the dendritic compartment of young visual neurons.

Dark-reared animals were examined to determine whether a low level of light through closed lids was more or less detrimental to the stability of dendritic PSD-95 than no visually driven activity. All procedures were as above except that 48 and 98 h levels were not measured. The decrease in PSD-95 at 96 h was not as prominent as that seen with eyelid suturing experiments, though it was still statistically significant (Fig. 5*B*). Thus, the lability of PSD-95 in central visual dendrites appears to be more sensitive to low levels of visual stimulation through closed eyelids than to the complete absence of visual stimulation in darkness.

Finally, we asked whether the ability to drop from high to low synaptoneurosome levels of PSD-95 in response to lack of visual stimulation was maintained into maturity. However, when the same suturing and reopening regime was applied to the eyes of P45 animals neither suturing or DR had an effect on synaptoneurosome levels of PSD-95 (Fig. 5 *C* and *D*).

Discussion

Our results suggest that PSD-95 becomes rapidly redistributed to the dendritic compartment within hours of EO in neurons of three visual centers. The increase in PSD-95 is temporally coincident with a similar increase in GKAP95. In addition, after, as compared with before EO, synaptoneurosomal PSD-95 is bound to more NR2A-rich NMDARs and less NR2B-rich NMDARs, but the amount of stargazin bound to PSD-95 remains constant. Finally, the increase in synaptoneurosome PSD-95 appears to be reduced in response to sensory deprivation in young but not in mature animals.

There is considerable evidence that light already drives the central visual neurons through the closed lids of rodents before EO (22, 23). Townsend *et al.* (24) has shown that a response similar, but smaller than the EO increase in synaptoneurosome PSD-95, is associated with increased NR2A subunit levels in the mouse sSC at an earlier stage of development when light first drives photoreceptors through closed lids (P8–P11). The earlier increase can be blocked by pharmacological disruption of the photoreceptor-to-ganglion cell pathway in the contralat-

eral eye (24). Thus, the phenomenon we describe is likely to represent a graded response of glutamatergic synapses to increases in retinal activation of central visual neurons regardless of whether the increase is caused by retinal circuit maturation or patterned and brighter light falling on the retinal surface after EO. Our examination of wl (Fig. 1) indicates that total PSD-95 increases with maturation at least in the juvenile period. A similar increase in PSD-95 has been noted in wl of the hippocampus (25). Our observation indicates that the synaptoneurosomal increase in PSD-95 is more attributable to its shifting distribution rather than to new protein synthesis during the 6-h period after EO. However, it is still plausible that some new protein synthesis is contributing to this increase. The latter observation and the finding that GKAP95 splice variants increase in dendritic fractions in parallel with PSD-95 suggest that the increase in dendritic PSD-95 may represent an activity-triggered redistribution of a PSD-95/GKAP95 complex to the dendritic domain. The postulate is consistent with a report that GKAPs associate with DLC, a light chain that can constitute a subunit of two motor proteins myosin Va and cytoplasmic dynein (26).

Retinal activity regulates developmental switches of NR subunits in dLGN (27) and NR2A subunit expression increases in VC after ferrets open their eyes (28). Increases in NR2A in VC synaptoneurosomes have also been documented 2 h after retrieval of P21 rats from DR (29). In addition, the rapid increase in NR2A at rat VC synapses will gradually decrease in five days after introduction of juvenile rats into darkness (30). The ages of the rats used and the timing of bidirectional changes in NR2A are similar to the current observations on PSD-95, and it is therefore plausible that the same trafficking mechanism may be involved. It is not clear, however, where the association between NR2A and PSD-95 actually takes place because the dendritic increase in NR2A is apparently blocked by cycloheximide (29), whereas we find that the increase in PSD-95 is not. The palmitoylation of PSD-95 (and not an association with transmembrane proteins) regulates its association with membrane vesicles and its postsynaptic targeting (31). Consequently, it is possible that NR2A synthesized locally is assembled into NR2A-rich NMDARs near the synapse. The NMDAR/PSD-95 complex could then be formed during fusion of PSD-95 and NMDAR containing vesicles in the subsynaptic region.

PSD-95 binds stargazin that increases the stability of AMPARs at synapses (3). Furthermore, overexpression of PSD-95 in dissociated hippocampal neurons results in an increase in the frequency and amplitude of spontaneous AMPAR currents as well as an increase in size and number of dendritic spines (32). The current data suggest that an activity-dependent redistribution of PSD-95 in dendrites could initiate a new phase of regulation for both NMDARs and AMPARs at central visual synapses.

In demonstrating a bidirectional modification of synaptic NMDARs, Philpot *et al.* (30) showed that visual deprivation after light exposure appears to reinstates a large number of NR2B-containing NMDARs at VC synapses. In the accompanying paper (24), we present evidence that NMDARs containing significant NR2B subunits remain in perisynaptic positions, where they make substantial contributions to evoked NMDAR currents, while new receptors enriched in NR2A and apparently associated with PSD-95 are inserted as clusters under glutamate release sites. In addition, NMDARs in cultured neurons have recently been shown to move laterally at synapses (33). In young animals, perisynaptic receptors may simply be able to move back to the centers of synapses when decreased visual activity causes the PSD-95 complex to leave the synapse. There may be molecules other than NR2A-rich NMDARs scaffolded exclusively by PSD-95 in visual neurons that are necessary for facilitating synaptic stability during activity-dependent synaptic competition. If this is the case, PSD-95's dendritic targeting and stability with pattern vision as well as its loss on visual deprivation may be an integral part of the mechanism allowing for ocular dominance plasticity in VC.

Finally, in the context of ocular dominance plasticity, it may be relevant that we find a smaller loss of PSD-95 in VC and sSC synaptoneurosomes when young (P16) rats are placed in total darkness for 4 days than if they simply have their eyes sutured shut in normal dark/light cycles for the same interval. Recently, the monocular deprivation paradigm has been used in kittens to show that the deprived eye is at a greater disadvantage in maintaining cortical synaptic space when it is sutured shut than when all of its activity is blocked by intraocular application of tetrodotoxin. The finding has led to the suggestion that weak visual activation of cortical synapses is more detrimental to successful synapse stabilization in the face of competition than no activity at all (34). We hypothesize that one of the first steps in monocular deprivation induced ocular dominance plasticity may be an ability of low levels of activity to remove PSD-95, NR2A rich NMDARs and associated signaling or stabilizing molecules from the postsynaptic densities of relatively inactive visual synapses.

We are grateful to Dr. Craig C. Garner for his generous donation of anti-SAP102 antibody. This research was supported by National Institute of Neurological Disorders and Stroke Grant R01NS32290 (to M.C.-P.) and National Eye Institute Grant R01EY06039 (to M.C.-P.).

1. Kornau, H. C., Schenker, L. T., Kennedy, M. B. & Seeburg, P. H. (1995) *Science* **269,** 1737–1740.
2. Garcia, E. P., Mehta, S., Blair, L. A., Wells, D. G., Shang, J., Fukushima, T., Fallon, J. R., Garner, C. C. & Marshall, J. (1998) *Neuron* **21,** 727–739.
3. Chen, L., Chetkovich, D. M., Petralia, R. S., Sweeney, N. T., Kawasaki, Y., Wenthold, R. J., Bredt, D. S. & Nicoll, R. A. (2000) *Nature* **408,** 936–943.
4. Husi, H., Ward, M. A., Choudhary, J. S., Blackstock, W. P. & Grant, S. G. (2000) *Nat. Neurosci.* **3,** 661–669.
5. Kennedy, M. B. (2000) *Science* **290,** 750–754.
6. Garner, C. C., Nash, J. & Huganir, R. L. (2000) *Trends Cell Biol.* **10,** 274–280.
7. Hollingsworth, E. B., McNeal, E. T., Burton, J. L., Williams, R. J., Daly, J. W. & Creveling, C. R. (1985) *J. Neurosci.* **5,** 2240–2253.
8. Scheetz, A. J., Nairn, A. C. & Constantine-Paton, M. (1997) *Proc. Natl. Acad. Sci. USA* **94,** 14770–14475.
9. Shi, J., Townsend, M. & Constantine-Paton, M. (2000) *Neuron* **28,** 103–114.
10. Cohen, R. S., Blomberg, F., Berzins, K. & Siekevitz, P. (1977) *J. Cell Biol.* **74,** 181–203.
11. Shi, J., Aamodt, S. M. & Constantine-Paton, M. (1997) *J. Neurosci.* **17,** 6264–6276.
12. Naisbitt, S., Kim, E., Weinberg, R. J., Rao, A., Yang, F. C., Craig, A. M. & Sheng, M. (1997) *J. Neurosci.* **17,** 5687–5696.
13. Lim, S., Naisbitt, S., Yoon, J., Hwang, J. I., Suh, P. G., Sheng, M. & Kim, E. (1999) *J. Biol. Chem.* **274,** 29510–29518.
14. Colonnese, M. T. & Constantine-Paton, M. (2001) *J. Neurosci.* **21,** 1557–1568.
15. Muller, B. M., Kistner, U., Kindler, S., Chung, W. J., Kuhlendahl, S., Fenster, S. D., Lau, L. F., Veh, R. W., Huganir, R. L., Gundelfinger, E. D. & Garner, C. C. (1996) *Neuron* **17,** 255–265.
16. Kim, E., Naisbitt, S., Hsueh, Y. P., Rao, A., Rothschild, A., Craig, A. M. & Sheng, M. (1997) *J. Cell Biol.* **136,** 669–678.
17. Pavlik, A. & Teisinger, J. (1980) *Brain Res.* **192,** 531–541.
18. Ouyang, Y., Rosenstein, A., Kreiman, G., Schuman, E. M. & Kennedy, M. B. (1999) *J. Neurosci.* **19,** 7823–7833.
19. Aakalu, G., Smith, W. B., Nguyen, N., Jiang, C. & Schuman, E. M. (2001) *Neuron* **30,** 489–502.
20. Scheetz, A. J., Nairn, A. C. & Constantine-Paton, M. (2000) *Nat. Neurosci.* **3,** 211–216.
21. Wells, D. G., Dong, X., Quinlan, E. M., Huang, Y. S., Bear, M. F., Richter, J. D. & Fallon, J. R. (2001) *J. Neurosci.* **21,** 9541–9548.

22. Fortin, S., Chabli, A., Dumont, I., Shumikhina, S., Itaya, S. K. & Molotchnikoff, S. (1999) *Brain Res. Dev. Brain Res.* **112,** 55–64.
23. Bansal, A., Singer, J. H., Hwang, B. J., Xu, W., Beaudet, A. & Feller, M. B. (2000) *J. Neurosci.* **20,** 7672–7681.
24. Townsend, M., Yoshii, A., Mishina, M. & Constantine-Paton, M. (2003) *Proc. Natl. Acad. Sci. USA* **100,** 1340–1345.
25. Sans, N., Petralia, R. S., Wang, Y. X., Blahos, J., 2nd, Hell, J. W. & Wenthold, R. J. (2000) *J. Neurosci.* **20,** 1260–1271.
26. Naisbitt, S., Valtschanoff, J., Allison, D. W., Sala, C., Kim, E., Craig, A. M., Weinberg, R. J. & Sheng, M. (2000) *J. Neurosci.* **20,** 4524–4534.
27. Ramoa, A. S. & Prusky, G. (1997) *Brain Res. Dev. Brain Res.* **101,** 165–175.
28. Roberts, E. B. & Ramoa, A. S. (1999) *J. Neurophysiol.* **81,** 2587–2591.
29. Quinlan, E. M., Philpot, B. D., Huganir, R. L. & Bear, M. F. (1999) *Nat. Neurosci.* **2,** 352–357.
30. Philpot, B. D., Sekhar, A. K., Shouval, H. Z. & Bear, M. F. (2001) *Neuron* **29,** 157–169.
31. El-Husseini, A. E., Craven, S. E., Chetkovich, D. M., Firestein, B. L., Schnell, E., Aoki, C. & Bredt, D. S. (2000) *J. Cell Biol.* **148,** 159–172.
32. El-Husseini, A. E., Schnell, E., Chetkovich, D. M., Nicoll, R. A. & Bredt, D. S. (2000) *Science* **290,** 1364–1368.
33. Tovar, K. R. & Westbrook, G. L. (2002) *Neuron* **34,** 255–264.
34. Rittenhouse, C. D., Shouval, H. Z., Paradiso, M. A. & Bear, M. F. (1999) *Nature* **397,** 347–350.